versus channels and time information, followed by a relatively short profile containing the occupancy information on the given frequency block during the five-minute monitoring period.

Another mode of operation is a monitor mode. It would provide for monitoring of a single channel at a high-sample rate. This optional mode of operation can be implemented relatively easily with minor programming. This mode is very useful in determining precisely what percentage of time a channel is occupied. This information can be of special significance for specific channels, such as emergency channels and/or other channels which show unusual occupancy conditions.

A more sophisticated application of the computer-controlled spectrum surveillance system is that of locating transmitters being used for bugging and eavesdropping. The frequency range and the mobility of the system allow it to be moved easily into buildings where suspected transmitters may be located. Cable coupling devices can be used to check power and telephone lines for transmission of information to some remote transmitter.

Only a few of the more apparent applications of the system have been discussed. As hardware is being deployed in the field, more and more applications are being generated, utilizing the mini-computer concept and data output compatible with batch processing computers. Changing from one application to another only requires additional software, thus minimizing the obsolescence of the system and maximizing the user's capital investment dollars.

References

[1] H. D. McKay and K. W. Bach, "Basic electromagnetic interference measurements on automobiles," presented at Soc. Automot. Eng., Automot. Eng. Cong., Detroit, Mich., Jan. 1971.

[2] A. W. DiMarzio, "Concept in computer control for frequency surveillance," *IEEE Trans. Aerosp. Electron. Syst.*, vol. AES-6, pp. 442–449, July 1970.

[3] K. W. Bach, "State-of-the-art in automatic and computer-controlled EMI measurements," Fairchild/Electro-Metrics Corp., Feb. 1970.

[4] H. D. McKay, "Current status electromagnetic pollution management and measurement," presented at IEEE Reg. Electromagnetic Compatibility Symp., Oct. 1970, Rec. 70-C-64-REGEMC.

A Discrete Point Approach to the Measurement of Radiated Power of Planar Apertures

AVINASH C. KAK, MEMBER, IEEE

***Abstract*—It is shown that for a high-gain circular aperture with linearly polarized and rotationally symmetric excitation the total real radiated power can be expressed as a weighted sum of radiation intensities in N direction, where N is equal to the first integer greater than $2.14D_\lambda$. D_λ is the diameter of the aperture in wavelengths. In an N-point measurement scheme the N directions and the weights involved in the weighted sum of radiation intensities are completely independent of the parameters of the radiation system and can be obtained from the well-known and tabulated properties of the Legendre polynomials. The criterion that N be equal to the first integer greater than $2.14D_\lambda$ is independent of any specific distribution in the aperture so long as it is of the type parabolic-on-a-pedestal. Such aperture distributions satisfy most needs and cover typical behavior of actual dish antennas. Even though the result of the threoretical formulation is that the above mentioned criterion for N holds good only for high directivity apertures, computational results show that for D_λ as small as 5 the error involved when N satisfies this criterion is less than 0.02 percent, and for D_λ equal to 7 the error reduces to 0.005 percent. This not only indicates that the criterion that N be equal to the first integer greater than $2.14D_\lambda$ holds good even for small values of D_λ, but it also shows the rapid decrease of error with increase in D_λ.**

A knowledge of the total radiated power is required for the determination of gain and radiation efficiency of an aperture. The discrete point approach to the measurement of total radiated power eliminates the need for using the conventional method of graphical integration of radiation patterns for the determination of the total radiated power. The method of graphical integration has been known to give erroneous results for high-gain apertures. Measurement of radiation intensities in the fine sidelobe structure is another source of error in the conventional method. In the discrete point approach the directions in which the radiation intensity need be measured tend to cluster around the normal to the aperture. This means fewer measurements in the fine sidelobe structure.

Manuscript received March 19, 1971; revised July 30, 1971.

The author is with the School of Electrical Engineering, Purdue University, Lafayette, Ind. 47907.

I. Introduction

THE TOTAL POWER radiated by an aperture is the integral of radiation intensity over all directions. In this paper we have shown that for circular apertures with rotationally symmetric excitation this integral for the total real radiated power can be given a discrete-point representation. We further show that this discrete-point representation can be of any order, but when the number of points is equal to or greater than $\|2.14D_\lambda\|$ for a high-gain aperture, ($D_\lambda \gg 1$) the error involved in such a representation is completely and entirely negligible. D_λ is the diameter of the aperture in wavelengths and $\|2.14D_\lambda\|$ denotes the first integer greater than the number $2.14D_\lambda$. Computational results show that even when D_λ is not very large the criterion that N be equal to $\|2.14D_\lambda\|$ holds good remarkably well. For example, for D_λ as small as 5 the error involved, when N is given by this criterion, is less than 0.02 percent. When D_λ is increased to 7 the error involved with N determined by the same criterion reduces to less than 0.005 percent. This also shows the rapid decrease of error as D_λ increases.

A consequence of this discrete-point representation is that for high-gain apertures the total real radiated power can be considered to be a weighted sum of radiation intensities in $\|2.14D_\lambda\|$ directions. This leads to the discrete-point approach to the measurement of total power radiated by an aperture. The directions in which the radiation intensity need be measured and the weights involved in the weighted sum of radiation intensities depend only upon the number of points in the measurement scheme, and are otherwise independent of the parameters of the radiation system. These directions and weights are completely determined by the properties of Legendre polynomials that are well known and extensively tabulated in the literature.

The criterion that for an N-point measurement scheme to be valid N must be equal to $\|2.14D_\lambda\|$ holds good regardless of any specific distribution in the aperture so long as it is of the type $(1-\rho^2)^n$-on-a-pedestal. These aperture distributions, also called parabolic-on-a-pedestal, satisfy most needs and cover typical behavior of actual dish antennas [1]. Whether the above stated rule would be true for Taylor circular apertures [2] also is still an open question. The mathematical expression of the pattern space factor of the Taylor-circular-aperture distribution appears to be too complicated for the type of analysis presented here. However, this does not reduce the range of applicability of our results as the Taylor distributions in large circular apertures are not readily realizable [1].

The theory that we have developed here holds good when the aperture fields are linearly polarized. This assumption is not overly restrictive, because for a wide class of practical aperture antennas the aperture fields can be considered to be almost completely linearly polarized, the energy in the cross-polarization component being almost completely negligible [3]. Our assumption of rotational symmetry of the aperture distributions is also not overly restrictive. The most common high-directivity apertures are of circular type, such as parabolic dishes. These apertures usually have rotationally symmetric aperture distributions. Although simple feeds like dipoles, slots, and horns have unequal E- and H-plane patterns, in practice considerable effort is expended to equalize the feed patterns in two planes [1].

The discrete-point approach to the measurement of total radiated power is shown to have advantages over the conventional methods. One conventional method consists of the experimental measurement of the radiation intensities in all directions and the graphical integration of the resulting power pattern [4]. The integration of power patterns is known to give results with error for high-gain apertures. The discrete-point approach eliminates this error entirely since there is no graphical integration involved. Measurement of radiation intensities in the fine sidelobe structure is another source of error in the conventional methods. In the discrete-point approach the directions in which the radiation intensity need be measured tend to cluster around the normal to the aperture. This means fewer measurements in the fine sidelobe structure.

II. A Discrete-Point Representation for the Radiated Power

For a planar aperture consisting of holes in a conducting screen in the yz plane the electromagnetic fields in the region $x>0$, the region into which the aperture radiates, can be expressed as a sum of an infinity of plane waves. By using the plane-wave spectrum representation the following expression for the total radiated power can be derived for an aperture the aperture electric field of which is polarized along the y axis. (By aperture electric field we mean the tangential component of electric field in the aperture [5]–[8]).

$$P_r = \frac{(2\pi)^2}{2\omega\mu_0} \iint_{(k_y^2+k_z^2)<k_0^2} \cdot \frac{(k_0^2 - k_z^2)\,|F_y(k_y, k_z)|^2}{(k_0^2 - k_y^2 - k_z^2)^{1/2}}\, dk_y\, dk_z \quad (1)$$

where $F_y(k_y, k_z)$ represents complex amplitude of the y component of the electric field in the continuous angular spectrum of plane waves, and can be obtained from the aperture electric field by the following relationship [5]–[8]

$$F_y(k_y, k_z) = \frac{1}{(2\pi)^2} \iint_S E_y(0, y, z) \cdot \exp\,[j(k_y y + k_z z)]\,dy\,dz \quad (2)$$

where $E_y(0, y, z)$ is the y component of the electric field in the aperture and S denotes the aperture surface. In (1) and (2) k_y and k_z are y and z components, respectively, of the free-space propagation vector of magnitude $k_0=\omega(\mu_0\epsilon_0)^{1/2}$. ω is the angular frequency, μ_0 the permeability, and ϵ_0 the dielectric constant of free space.

In a spherical coordinate system, the polar axis of which coincides with the normal to the aperture, the expression (1) for the total radiated power can be shown to transform into

$$P_r = \frac{(2\pi)^2 k_0^3}{2\omega\mu_0} \int_0^1 \int_0^{2\pi} \frac{t(1 - t^2 \sin^2 \phi)}{\sqrt{(1 - t^2)}}\, |F_y(t, \phi)|^2 d\phi\, dt \quad (3)$$

where $t=\sin\theta$. Note that the polar angle θ is measured from the normal to the aperture. φ is the azimuthal angle, and is measured in the plane of the aperture from the z axis. In this spherical coordinate system the following relationship can also be derived

$$E_y(R, \theta, \phi) = \frac{j2\pi k_0 \cos\theta}{R} \exp(-jk_0 R) F_y(\theta, \phi) \quad (4)$$

where R is the distance from the origin. This relationship, which holds only in the far-field region, can be derived by applying the method of stationary phase to the plane-wave spectrum representation of $E_y(x, y, z)$ [9].

For circular apertures with rotationally symmetric excitation F_y, given by (2), reduces to the zeroth order Hankel transform of the y component of electric field in the aperture and is independent of the azimuthel angle φ. Therefore, expression (3) for total radiated power reduces to

$$P_r = \int_0^1 \frac{1}{\sqrt{1-t}} h(t)\, dt \quad (5)$$

where

$$h(t) = \frac{(2\pi)^3 k_0^3}{2\omega\mu_0} \frac{(1 - t^2/2)t}{\sqrt{(1+t)}} \,|\, F_y(t) \,|^2. \quad (6)$$

For all aperture distributions that we shall be concerned with, $|F_y(t)|^2$, and therefore $h(t)$, possess derivatives of all orders on the interval (0, 1). This implies that if we give a discrete N-point representation to the integral in (5) by the theorem presented in Appendix I, then it is possible to calculate the error involved in such a representation for any value of N, since for every N the function $h(t)$ possesses the $(2N)$th derivative in the interval (0, 1). Therefore, by the theorem in Appendix I, we can write (5) as

$$P_r = \sum_{k=1}^{N} \alpha_k h(t_k) + \frac{2^{4N+1}}{4N+1} \frac{[(2N)!]^3}{[(4N)!]^2} h^{(2N)}(\eta) \quad (7)$$

where $0 < \eta < 1$. The second term on the right-hand side in (7) denotes the error involved in the discrete-point representation and will be called the error term. t_k and α_k are given by

$$t_k = 1 - \xi^2_{k,2N} \quad (8)$$

$$\alpha_k = 2\alpha_{k,2N} \quad (9)$$

$\xi_{k,2N}$ is the kth positive zero of the Legendre polynomial of degree $2N$, the zeros being counted from the one which is closest to $+1$. $\alpha_{k,2N}$ is the weight corresponding to $\xi_{k,2N}$ in the Gauss–Legendre quadrature rule of order $2N$. Both $\xi_{k,2N}$ and the corresponding $\alpha_{k,2N}$ have been tabulated by Stroud and Secrest [10] for values of $(2N)$ up to 516. It should be noted that all t_k lie between 0 and 1.

It was indicated in the Introduction that we are concerned here with high-directivity circular apertures with aperture excitation of the type parabolic-on-a-pedestal. Let D_λ denote the diameter of such an aperture in wavelengths. In the next section an upper bound for the error term in (7) is derived and it is shown that for such apertures if $D_\lambda \gg 1$, and if $N > 2.14 D_\lambda$ then the error term in (7) becomes entirely negligible and can be taken to be zero for all purposes. And, in fact, N need only be equal to $\|2.14D_\lambda\|$, where $\|2.14D_\lambda\|$ denotes the first integer greater than the number $2.14D_\lambda$. Computational results presented in Section IV show that even when D_λ is as small as 7 the error term, when $N = \|2.14D_\lambda\|$, is of the order of $10^{-5}P_r$ which is indeed negligible for all engineering purposes. The error term is also shown to decrease very rapidly as D_λ increases. It should be noted that the criterion that $N = \|2.14D_\lambda\|$ is independent of the aperture distribution so long as it is of the type parabolic-on-a-pedestal. Therefore, we can write

$$P_r = \sum_{k=0}^{\|2.14D_\lambda\|} \alpha_k\, h(t_k) \quad (10)$$

where we have retained the equality sign to emphasize that the error involved is an entirely negligible fraction of P_r for high-gain apertures.

Substituting (4) in (6), and substituting the resulting equation in (10), we get, after making use of the fact that $t = \sin\theta$,

$$P_r = 2\pi \sum_{k=0}^{N} \beta_k \left[\frac{R^2}{2Z_0} \,|\, E_y(R, \theta_k) \,|^2 \right] \quad (11)$$

where

$$N = \|2.14D_\lambda\|$$

$$\beta_k = \alpha_{k,2N} \frac{(2 - \sin^2\theta_k)}{\sqrt{(1 + \sin\theta_k)}} \frac{\sin\theta_k}{\cos^2\theta_k} \quad (12)$$

$$\theta_k = \sin^{-1}(t_k) = \sin^{-1}(1 - \xi^2_{k,2N}) \quad (13)$$

$$Z_0 = \sqrt{(\mu_0/\epsilon_0)}.$$

As has been mentioned before $\xi_{k,2N}$ and α_{k12N} have been tabulated by Stroud and Secrest [10] for each value of $2N$ up to 512. By using (12) and (13) it is indeed a simple matter to convert these tables into θ_k, β_k tables for each value of N up to 256.

In (11) $R^2/2Z_0 \cdot |E_y(R, \theta_k)|^2$ represents the radiation intensity as determined from y-directed component of electric field alone in the direction θ_k in the far-field region. The angle θ_k is measured from the normal to the aperture, and the azimuthal angle does not matter because of rotational symmetry.

Equation (11) represents the total radiated power as a sum of radiation intensities, as determined from only one component of the electric field, in $\|2.14D_\lambda\|$ directions. That only one component of electric field is involved in the discrete sum is not at all surprising. That is because it is quite possible to express the conventional integral for the total radiated power in terms of only the y component of electric field in the far-field region [11].

III. Error Estimate for the Discrete-Point Representation

In this section our aim is to justify (10). In other words, we have to show that the error term in (7) is indeed a vanishingly negligible fraction of total radiated power when $N = \|2.14D_\lambda\|$.

Let the error term in (7) be denoted by $E_N(P_r)$, then

$$E_N(P_r) = \frac{2^{4N+1}}{4N+1} \frac{[(2N)!]^3}{[(4N)!]^2} h^{(2N)}(\eta) \tag{14}$$

where $0<\eta<1$. This means that there exists a point in the interval (0, 1) at which the $(2N)$th derivative of $h(t)$ yields through (14) the required error. Now suppose we are able to find a quantity M_{2N} that is an upper bound on the magnitude of the $(2N)$th derivative of $h(t)$ on the interval (0, 1), then

$$| h^{(2N)}(\eta) | \leq M_{2N} \tag{15}$$

and we can write for the upper bound on the $|E_N(P_r)|$

$$| E_N(P_r) | \leq \frac{2^{4N+1}}{4N+1} \frac{[(2N)!]^3}{[(4N)!]^2} M_{2N}. \tag{16}$$

In the subsequent analysis we will determine the quantity M_{2N} and, thence, the upper bound on the error $|E_N(P_r)|$.

As was mentioned in the Introduction, our concern here is with the aperture excitation of the type parabolic-on-a-pedestal. Expressed mathematically for a circular aperture of radius L, the aperture electric field can be written as

$$\begin{aligned} E_y(0, y, z) &= E_{y0}\{b + [1 - (\rho/L)^2]^n\}, \qquad \rho \leq L \\ &= 0, \qquad \rho > L \end{aligned} \tag{17}$$

where b controls the height of the pedestal and n is any integer greater than zero. In the above equation ρ is given by

$$\rho = \sqrt{(y^2 + z^2)}. \tag{18}$$

The y component of the pattern-space factor of such an aperture distribution is obtained by substituting (17) in (2). We get

$$F_y(t) = E_{y0}L^2 \frac{1}{4\pi} \left[b\Lambda_1(k_0Lt) + \frac{\Lambda_{n+1}(k_0Lt)}{n+1} \right] \tag{19}$$

where

$$\Lambda_n(x) = \frac{n! J_n(x)}{(x/2)^n} \tag{20}$$

$J_n(x)$ being the nth-order Bessel function.

Substituting (19) in (6), we can write for $h(t)$

$$h(t) = \left[\frac{E_{y0}L^2}{2}\right]^2 \frac{\pi k_0^3}{\omega\mu_0} \frac{(1 - t^2/2)t}{\sqrt{(1+t)}} \cdot \left[b\Lambda_1(k_0Lt) + \frac{\Lambda_{n+1}(k_0Lt)}{n+1} \right]^2. \tag{21}$$

The t-dependent term outside the square brackets, i.e.,

$$\frac{(1 - t^2/2)t}{\sqrt{(1+t)}}$$

is a relatively smooth (nonoscillatory) function in the interval (0, 1). A plot of this function would show that its value increases without changing sign from zero at the origin to 0.35 to $t=1$, attaining a maximum of 0.40 at approximately $t=0.8$. (Apparently the singularity of this function, which occurs at $t=-1$, is too far away from the interval (0, 1) to effect the smooth nature of the function in this interval.) In sharp contrast to this the function inside the square brackets in (21) becomes highly oscillatory in the interval (0, 1) for high-directivity apertures. For these apertures $k_0L(\equiv \pi D_\lambda) \gg 1$. Then by the arguments presented in Appendix II we can obtain a good estimate for M_{2N}, which is an upper bound on $|h^{(2N)}(t)|$, from the upper bound on

$$\left[\frac{E_{y0}L^2}{2}\right]^2 \frac{\pi k_0^3}{\omega\mu_0} \frac{(1 - t^2/2)t}{\sqrt{(1+t)}} \cdot \left| \left[\left(b\Lambda_1(k_0Lt) + \frac{\Lambda_{n+1}(k_0Lt)}{n+1} \right)^2 \right]^{(2N)} \right|, \quad 0 \leq t \leq 1 \tag{22}$$

we will first determine an upper bound on $|g^{(2N)}(t)|$ where $g(t)$ is given by

$$g(t) = \left(b\Lambda_1(k_0Lt) + \frac{\Lambda_{n+1}(k_0Lt)}{n+1} \right)^2, \qquad 0 \leq t \leq 1. \tag{23}$$

Expanding the right-hand side of (23), taking the $(2N)$th derivative of both sides, and employing the elementary principles of analysis, we get

$$\begin{aligned} | g^{(2N)}(t) | \leq b^2 | \{[\Lambda_1(k_0Lt)]^2\}^{(2N)} | &+ \left| \left\{ \left[\frac{\Lambda_{n+1}(k_0Lt)}{n+1} \right]^2 \right\}^{(2N)} \right| \\ &+ 2b \left| \left[\Lambda_1(k_0Lt) \cdot \frac{\Lambda_{n+1}(k_0Lt)}{n+1} \right]^{(2N)} \right|, \\ &\qquad 0 \leq t \leq 1. \end{aligned} \tag{24}$$

Upper bounds for each of the three terms on the right-hand side of (24) can be found by giving appropriate values to the parameters p and q in the inequality (43) in Appendix III. When these upper bounds are substituted in (24), we get

$$\begin{aligned} | g^{(2N)}(t) | \leq \frac{2^{4N+2}e^2}{\pi N^3} \left[\frac{k_0L}{2}\right]^{2N} &\cdot [b^2 + (2e/N)^{2n}(n!)^2 + 2b(2e/N)^n(n!)], \\ &\qquad 0 \leq t \leq 1 \end{aligned} \tag{25}$$

where e is the base of natural logrithm. For the other t-dependent factor in (21) it is a simple matter to show that

$$\frac{(1 - t^2/2)t}{\sqrt{(1+t)}} < 0.5, \qquad 0 \leq t \leq 1. \tag{26}$$

In the arguments leading to (22) it was pointed out that a good estimate for M_{2N}, which is an upper bound on $|h^{(2N)}(t)|$ in the interval $0<t<1$, could be obtained from the upper bound on (22). Recalling the definition of $g(t)$ as given by (23), and making use of (25) and (26), we can write

$$M_{2N} = \left(\frac{E_{y0}L^2}{2}\right)^2 \frac{k_0^3}{2\omega\mu_0} \frac{2^{4N+2}e^2}{N^3} \left(\frac{k_0L}{2}\right)^{2N} \cdot [b^2 + (2e/N)^{2n}(n!)^2 + 2b(2e/N)^n(n!)]. \quad (27)$$

Substituting (27) in (16), we get

$$| E_N(P_r) | \leq \left(\frac{E_{y0}L^2}{2}\right)^2 \frac{k_0^3e^2}{2\omega\mu_0} \frac{2^{8N+3}}{N^3(4N+1)} \frac{[(2N)!]^3}{[(4N)!]^2} \cdot \left[\frac{k_0L}{2}\right]^{2N} \cdot [b^2 + (2e/N)^{2n}(n!)^2 + 2b(2e/N)^n(n)!]. \quad (28)$$

For $D_\lambda \gg 1$ we certainly expect $N \gg 1$. This suggests that (28) can be simplified by using Stirling's approximation for the factorials involving N. By Stirling's approximation when k is larger

$$k! \simeq \sqrt{2\pi} k^{k+1/2} e^{-k}. \quad (29)$$

To illustrate the order of approximation involved, 10! when computed by the above formula yields 3.598×10^6 while the actual value is 3.628×10^6.

Employing Stirling's approximation in (28) we get

$$\frac{| E_N(P_r) |}{[P_r]_{OM}} \leq \frac{8}{\sqrt{\pi}} \frac{1}{N^{3/2}} \left[\frac{2.14D_\lambda}{N}\right]^{2N+2} \cdot [b^2 + (2e/N)^{2n}(n!)^2 + 2b(2e/N)^n(n!)] \quad (30)$$

where we have used $(\pi e/4) \simeq 2.14$, and

$$[P_r]_{OM} = \frac{E_{y0}^2}{2Z_0} \pi L^2. \quad (31)$$

In practice the value of b lies between 0 and 1, while that of n lies between 1 and 5, (see [12]). For these values of b and n, $[P_r]_{OM}$ represents the order-of-magnitude of total real power radiated.

Since both b and n are of order unity, an examination of the right-hand side of (30) reveals that for

$$D_\lambda \gg 1$$

and

$$N > 2.14D_\lambda$$

the $|E_N(P_r)|/[P_r]_{OM}$ is completely and entirely negligible. And in fact for high-gain apertures N need only be equal to $\|2.14D_\lambda\|$, the first integer greater than $2.14D_\lambda$, for the error to be vanishingly small. This justifies (10).

IV. Some Computational Results

A principal assumption made in the derivation of error estimate presented in Section II was that $D_\lambda \gg 1$. As a consequence of this assumption M_{2N} was obtained from the upper bound on (22) and, also, Stirling's approximation could be used for the factorials of N. And indeed greater the D_λ is the greater justification for employing these simplications.

In the light of the above statement it becomes of considerable interest to know how well the criterion $N = \|2.14D_\lambda\|$ fares for apertures for which D_λ cannot exactly be considered to be very much greater than unity. In what follows we will consider two cases belonging to this class, i.e., $D_\lambda = 5$ and $D_\lambda = 7$ wavelengths, and show that the formula $N = \|2.14D_\lambda\|$ for the error involved in the discrete-point representation to be negligible holds remarkably true even in these cases. The two values of D_λ were taken to show the rapid decrease in the error involved as D_λ is increased from 5 to 7.

Substituting (21) and (31) in (7), we can write for the total power radiated

$$\frac{P_r}{[P_r]_{OM}} = \frac{\pi^2 D_\lambda^2}{2} \sum_{k=1}^{N} \alpha_k \cdot \frac{(1 - t_k^2/2)t_k}{\sqrt{(1+t_k)}} \cdot \left(b\Lambda_1(\pi D_\lambda t_k) + \frac{\Lambda_{n+1}(\pi D_\lambda t_k)}{n+1}\right)^2 + \text{error term} \quad (32)$$

where we have normalized P_r by dividing it by $[P_r]_{OM}$, and where we have written error term for the second term on the right-hand side for (7). As has been explained in Section II, it is a simple matter to generate (α_k, t_k) tables from the tables provided by Stroud and Secrest [10]. This was done on a digital computer for each value of N from 10 to 20.

For the purpose of computation n was given a value of unity. For each value of D_λ, b was given three values 0, 0.25, and 0.5. The series on the right-hand side of (32) was summed for each value of D_λ and b, and the result multiplied by the factor $\pi^2 D_\lambda^2/2$ occurring in (32). Numerical results correct to five decimal places have been presented in Tables I and II.

To understand Tables I and II it is necessary to bear in mind that as N is increased in (32), the error term decreases and would be practically zero after N has reached a certain value. The value of the summation for this value of N is the true value of normalized power. For example, we see from Table I that for $D_\lambda = 5$ there is no change in the value of normalized P_r as N is increased from 15 onwards. Therefore, we can say that for $D_\lambda = 5$ and $b = 0.5$ the *true* value of normalized power is 1.07658, and the magnitude of error involved in using a discrete 11-point (which corresponds to $N = \|2.14D_\lambda\|$ in this case) representation is 2×10^{-4}, which is less than 0.02 percent. For the same value of b when D_λ is increased to 7 (see Table II), the $N = \|2.14D_\lambda\| (\equiv 15)$ representation gives an error of 5×10^{-5}, which is less than 0.005 percent. Note the rapid decrease in error involved with a small increase in D_λ.

Therefore, we can say that the criterion that $N = \|2.14D_\lambda\|$ for the discrete-point representation to be valid is not really limited by the assumption that D_λ be very much greater than unity.

V. Applications of the Theory

We have the conclusion that for high-directivity circular apertures with linearly polarized and rotationally symmetric excitation the total real radiated power can be considered to be a weighted sum of radia-

TABLE I

N	Normalized total radiated power as obtained by summing the series on the R.H.S. of equation (32) for $D_\lambda = 5$, $n = 1$, and		
	b = 0.5	b = 0.25	b = 0
10	1.07538	0.64371	0.33319
11	1.07673	0.64428	0.33330
12	1.07656	0.64422	0.33328
13	1.07658	0.64421	0.33328
14	1.07658	0.64421	0.33328
15	1.07658	0.64421	0.33328
16	1.07658	0.64421	0.33328
17	1.07658	0.64421	0.33328
18	1.07658	0.64421	0.33328
19	1.07658	0.64421	0.33328
20	1.07658	0.64421	0.33328

TABLE II

N	Normalized total radiated power as obtained by summing the series on the R.H.S. of equation (32) for $D_\lambda = 7$, $n = 1$ and		
	b = 0.5	b = 0.25	b = 0
10	1.04260	0.63433	0.33494
11	1.09811	0.65130	0.33354
12	1.07175	0.64218	0.33311
13	1.07988	0.64520	0.33338
14	1.07801	0.64449	0.33330
15	1.07835	0.64463	0.33332
16	1.07830	0.64460	0.33331
17	1.07831	0.64461	0.33331
18	1.07830	0.64461	0.33331
19	1.07830	0.64461	0.33331
20	1.07830	0.64461	0.33331

tion intensities in $\|2.14D_\lambda\|$ directions. For a given N-point measurement scheme, the weights and the directions involved are completely independent of the parameters of the radiation system, and can be obtained from the well-known properties of Legendre polynomials that have been tabulated by various authors. And, also, for determining the radiation intensities that enter the weighted sum, only one component of the electric field in the far-field region need be measured.

A knowledge of radiated power is required for the computation of gain and radiation efficiency. The conventional method that is usually employed to determine the total radiated power consists of measuring radiation intensities in all directions in space and the graphical integration of the resulting power pattern [4]. The determination of radiated power of high-directivity aper-

TABLE III

Sin θ_k for a 20-Point Representation of the Radiated Power

k	Sin θ_k
1	0.003
2	0.018
3	0.044
4	0.082
5	0.129
6	0.186
7	0.250
8	0.320
9	0.394
10	0.471
11	0.548
12	0.624
13	0.698
14	0.766
15	0.828
16	0.883
17	0.928
18	0.962
19	0.986
20	0.998

tures by this method has generally been found to be difficult. Two of the difficulties follow.

1) The error introduced into the graphical integration of the power patterns of such apertures.

2) The error introduced in measuring the fine sidelobe structure.

Our representation of the radiated power eliminates the first difficulty entirely, since the graphical integration is replaced by a sum of radiation intensites (as determined from only one component of electric field in the far-field region).

The discrete approach also reduces the second difficulty.[1] That this is so will be explained with the help of an example in which we will consider a discrete-point representation of order 20. Although for high-directivity aperture's higher order discrete-point representations are called for, it would mean presenting a huge amount of data not necessarily leading to any additional insight. For $N=20$, $\sin\theta_k(\equiv t_k)$ were computed from the zeros of the Legendre polynomial of degree 40 by the method discussed in Section II. The values of $\sin\theta_k$ obtained have been presented in Table III. From these values of $\sin\theta_k$ we can see that for $N=20$, the first thirteen θ_k lie between 0° and 45°, while only the last seven are between 45° and 90°. Now if it is recognized that the angular interval 0° to 45° contains the main beam and the first few sidelobes, and as θ approaches 90° the sidelobe structure becomes finer, then it is clear that fewer measurements need be made in the region where sidelobe structure is very fine. The property of θ_k to cluster around the normal to the aperture is a consequence of the fact that the positive zeros of a Legendre poly-

[1] Further work is required to determine the extent to which the second difficulty is reduced. That is because even though the number of measurements in the fine sidelobe structure would be very small compared to the number of measurements in the main beam, the overall accuracy would still be influenced by the accuracy of measurements in the sidelobe structure, and further work is necessary to determine the extent of this influence.

nomial approach $+1$ (they remain distinct, of course) as the degree of the polynomial approaches infinitity [13]. The clustering of θ_k around the normal to the aperture becomes more pronounced as N is increased.

In addition to determining radiated power from a discrete set of measurements some new measurement techniques are suggested by our approach. For example, if at a test site or in an antenna test chamber, N dipoles were fixed at angles θ_k that can easily be calculated from our theory, then these fixed dipoles would measure the total radiated power of *all* rotationally symmetric apertures with diameters less than $N/2.14$ wavelengths. That is because the angles at which the radiation intensity need be measured depend only upon the total number of points in the measurement scheme and not on the diameter of the aperture. And the number of points can be any value greater than $2.14D_\lambda$.

Appendix I

The discrete-point representation of integrals is the result of Gauss–Jacobi theory of quadratures. An excellent treatment of the foundations of this theory can be found in the book by Davis [13]. In what follows we will present a theorem without proof. For proof see Krylov *et al.* [14] and Davis and Rabinowitz [15].

Theorem

Let $f(x)$ belong to the class of functions that are at least $2N$-times differentiable in the interval (0, 1) then

$$\int_0^1 \frac{1}{\sqrt{(1-x)}} f(x)\,dx = \sum_{k=1}^{N} \alpha_k f(x_k) + \frac{2^{4N+1}}{4N+1} \frac{[(2N)!]^3}{[(4N)!]^2} f^{(2N)}(\eta) \quad (33)$$

where $0<\eta<1$. Here $x_k = 1-\xi^2_{k,2N}$, where $\xi_{k,2N}$ is the kth zero of the Legendre polynomial of the degree $2N$, the first zero being the one which is closest to $+1$. All x_k lie between 0 and $+1$. $\alpha_k = 2\alpha_{k,2N}$, where $\alpha_{k,2N}$ is the weight corresponding to $\xi_{k,2N}$ in the $(2N)$th-order Gauss–Legendre quadrature rule.

$\alpha_{k,2N}$ and the corresponding $\xi_{k,2N}$ have been tabulated by Stroud and Secrest [10] for each value of $2N$ up to 512. From these it is a simple matter to generate x_k, α_k tables for any value of N up to 256.

Appendix II

In this appendix we will illustrate that if a function is a product of a relatively smooth (nonoscillatory) part and a highly oscillatory part, then a good estimate for the upper bound of the Kth derivative of the function over a given interval is the product of the upper bound on the nonoscillatory part and the upper bound on the Kth derivative of the oscillatory part over the interval.

Consider for example,

$$f(x) = \frac{x^2}{1+x} \sin ax, \qquad a \gg 1 \quad (34)$$

over the interval $0<x<1$. Consider, for example, the second derivative of this function over the interval $0<x<1$. Taking the second derivative and using the elementary principles of analysis, we can write

$$\max_{0<x<1} |f^{(2)}(x)| \le \max_{0<x<1} \left| \frac{2}{1+x}\left[1 - \frac{2x}{1+x} + \frac{x^2}{(1+x)^3}\right] \sin ax \right| + \max_{0<x<1} \left| 2\left[\frac{2x}{1+x} - \frac{x^2}{(1+x)^2}\right] a \cos ax \right| + \max_{0<x<1} \left| \frac{x^2}{1+x} a^2 \sin ax \right|. \quad (35)$$

Since $a \gg 1$, it is easy to see that the first and the second terms are of the order $(1/a^2)$ and $(1/a)$, respectively, of the third term and can, therefore, be neglected in comparison with the third term. Therefore, when $a \gg 1$, it is a good approximation to write

$$\max_{0<x<1} |f^{(2)}(x)| \le \max_{0<x<1} \left| \frac{x^2}{1+x^2} a^2 \sin ax \right|. \quad (36)$$

The right-hand side of (36) has the following upper bound

$$\max_{0<x<1} \left| \frac{x^2}{1+x^2} \right| \cdot \max_{0<x<1} |(\sin ax)^{(2)}| \quad (37)$$

which proves the statement made at the beginning of the Appendix. Similar arguments would hold if the sine function in (34) is replaced by a Bessel function which is highly oscillatory in the interval under consideration.

Appendix III

The series expansion for the product $J_p(ax)J_q(ax)$ is given by [16]

$$J_p(ax)\,J_q(ax) = \sum_{m=0}^{\infty} \frac{(-1)^m (ax/2)^{p+q+2m} (p+q+2m)!}{m!(p+q+m)!(p+m)!(q+m)!}. \quad (38)$$

J_p and J_q are Bessel functions of order p and q, respectively. Now

$$\frac{\Lambda_p(ax)}{p} \frac{\Lambda_q(ax)}{q} = (p-1)!(q-1)!(2/ax)^{p+q} J_p(ax) J_q(ax). \quad (39)$$

Substituting (38) in (39) and taking $(2N)$th derivative of both sides, we get

$$\left[\frac{\Lambda_p(ax)}{p} \frac{\Lambda_q(ax)}{q}\right]^{(2N)} = (p-1)!(q-1)! \sum_{m=0}^{\infty} \frac{(-1)^{m+N}(p+q+2m+2N)!(2m+2N)!(a/2)^{2m+2N} x^{2m}}{(m+N)!(p+q+m+N)!(p+m+N)!(q+m+N)!(2m)!}. \quad (40)$$

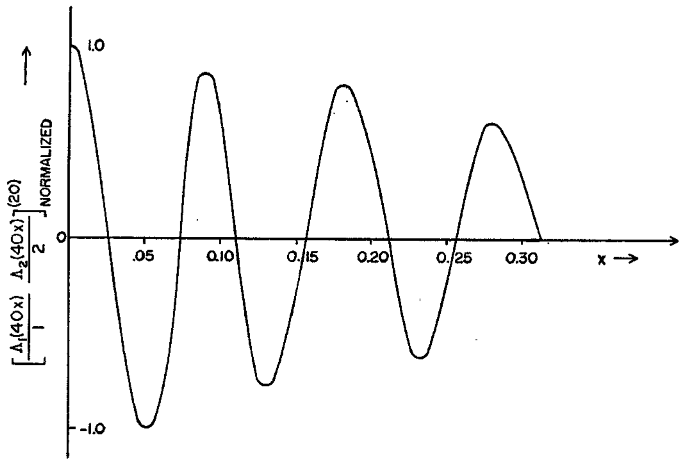

Fig. 1. Graph of the normalized value of $[\Lambda_p(ax)/p\ \Lambda_q(ax)/q]^{(2N)}$ for $p=1$, $q=2$, $a=40$, and $N=20$.

The series in (40) was summed on a digital computer for various values of p, q, a, and N. For each set of the values of p, q, a, and N the result obtained indicates an oscillatory function which has a maximum amplitude at $x=0$. The amplitude of oscillations decreases to zero as x becomes very large. For illustration Fig. 1 shows the graph obtained for

$$\frac{\left[\frac{\Lambda_p(ax)}{p}\ \frac{\Lambda_q(qx)}{q}\right]^{(2N)}}{\left[\frac{\Lambda_p(ax)}{p}\ \frac{\Lambda_q(ax)}{q}\right]^{(2N)}_{\text{at } x=0}} \tag{41}$$

for $p=1$, $q=2$, $a=40$, and $N=20$ and for $0<x<0.3$. Therefore, we can write

$$\left|\left[\frac{\Lambda_p(ax)}{p}\ \frac{\Lambda_q(ax)}{q}\right]^{(2N)}\right| \le (p-1)!(q-1)! \cdot \frac{(p+q+2N)!(2N)!(a/2)^{2N}}{N!(p+q+N)!(p+N)!(q+N)!} \tag{42}$$

the right-hand side being obtained by putting $x=0$ in (40). For high-directivity apertures where $D_\lambda \gg 1$ we certainly expect $N \gg 1$. Therefore, we can use Stirling's approximation [see (29)] for those factorials in (42) the argument of which contains N. We get

$$\left|\left[\frac{\Lambda_p(ax)}{p}\ \frac{\Lambda_q(ax)}{q}\right]^{(2N)}\right| \le \frac{1}{\pi}\ \frac{2^{4N+2}e^2(a/2)^{2N}}{N^3} \cdot (2e/N)^{p+q-2}(p-1)!(q-1)!. \tag{43}$$

In obtaining (43) we have assumed p and q are small compared with N. This is indeed the case in Section III where this inequality is to be used.

References

[1] R. C. Hansen, *Microwave Scanning Antennas*, vol. 1. New York: Academic Press, 1964, ch. 1.
[2] T. T. Taylor, "Design of circular apertures for narrow beam-width and low sidelobes," *IEEE Trans. Antennas Propagat.*, vol. AP-8, pp. 17–22, Jan. 1960.
[3] S. Silver, *Microwave Antenna Theory and Design.* New York: McGraw-Hill, 1949.
[4] "IEEE test procedure for antennas, no. 149," *IEEE Trans. Antennas Propagat.*, vol. AP-13, pp. 437–466, May 1965.
[5] R. E. Collin and S. Rothschild, "Reactive energy in aperture fields and aperture Q," *Can. J. Phys.*, vol. 41, pp. 1967–1979, Dec. 1963.
[6] G. Borgiotti, "Fourier transforms method of aperture antennas problems" (in English), *Alta Freq.*, vol. 32, pp. 196–204, Nov. 1963.
[7] G. Borgiotti, "Radiation and reactive energy of aperture antennas," *IEEE Trans. Antennas Propagat.* (Commun.), vol. AP-11, pp. 94–95, Jan. 1963.
[8] D. R. Rhodes, "On the stored energy of planar apertures," *IEEE Trans. Antennas Propagat.*, vol. AP-14, pp. 676–683, Nov. 1966.
[9] D. R. Rhodes, "On a fundamental principle in the theory of planar antennas," *Proc. IEEE*, vol. 52, pp. 1013–1021, Sept. 1964.
[10] A. H. Stroud and D. Secrest, *Gaussain Quadrature Formulas.* Englewood Cliffs, N. J.: Prentice-Hall, 1966.
[11] A. C. Kak, "On the Rhodes' principle in the theory of planar antennas," *Int. J. Electron.*, vol. 28, no. 2, pp. 143–148, 1970.
[12] J. P. Grantham, "Secondary characteristics of the circular aerial for a range of theoretical uniphase aperture distributions," ASRE, Portsmouth, England, Tech. Note NX-53-2.
[13] P. Davis, *Interpolation and Approximation.* Waltham, Mass.: Blaisdell, 1963.
[14] V. I. Krylov, V. V. Lugin, and L. A. Ianovich, *Tables for the Numerical Integration of Functions with Power Singularities.* Moscow, USSR, 1963.
[15] P. Davis and P. Rabinowitz, *Numerical Integration.* Waltham, Mass.: Blaisdell, 1967, p. 75.
[16] G. N. Watson, *A Treatise on the Theory of Bessel Functions.* New York: Cambridge Press, 1914.